Angle of Arrival Fluctuations for Free Space Laser Beam Propagation through non Kolmogorov turbulence

Italo Toselli[a], Larry. C. Andrews[b], Ronald L. Phillips[c], Valter Ferrero[a]

[a]Optical Communications Group, Politecnico di Torino, 10128 Turin, Italy
[b]Department of Mathematics, University of Central Florida, Orlando, FL32816
[c]University of Central Florida, Florida Space Institute, MS: FSI, Kennedy Space Center, FL 32899

ABSTRACT

Atmospheric turbulence induces significant variation on the angle-of-arrival of laser beams used in free space laser communication. Angle-of-arrival fluctuations of an optical wave in the plane of the receiver aperture can be described in terms of the phase structure function that already has been calculated by Kolmogorov's power spectral density model. Unfortunately several experiments showed that Kolmogorov theory is sometimes incomplete to describe atmospheric statistics properly. In this paper, for horizontal path and weak turbulence, we carry out analysis of angle-of-arrival fluctuations using a non Kolmogorov power spectrum which uses a generalized exponent factor instead of constant standard exponent value 11/3 and a generalized amplitude factor instead of constant value 0.033. Also our non Kolmogorov spectrum includes both inner scale and outer scale effects.

Keywords: Atmospheric turbulence, structure function, non Kolmogorov spectrum, angle of arrival.

1. INTRODUCTION

Since it has been introduced Kolmogorov's power spectral density model has been widely used and accepted to describe wave propagation through atmospheric turbulence. It has been already used also to calculate free space laser system performance that is limited by atmospheric turbulence. However, recent experimental data from space-based stellar scintillation, balloon-borne in-situ temperature, and ground-based radar measurements indicate turbulence in the upper troposphere and stratosphere deviates from predictions of the Kolmogorov model [5][9][10]. Further development of the turbulent theory of passive scalar transfer has shown that although the Kolmogorov spectrum is important, it constitutes only one part of the more general behavior of passive scalar transfer in a turbulent flow [6]. Some anomaly behavior [3] seem to occur when the atmosphere is extremely stable because under such condition the turbulence is no longer homogeneous in three dimensions since the vertical component is suppressed. It has been shown [4] that for such two dimensional turbulence, coherent vortices can develop that reduce rate of the energy cascade from larger to smaller scales. As a result Kolmogorov turbulence will not develop. In addition anisotropy in stratospheric turbulent inhomogeneities has been experimentally investigated [5][8][11][12]. We must accept de facto that turbulence is still an unsolved problem in classical physics and the scientific community must persist in doing more simulations, measurements and experiments [7].

It is very important, therefore, to find new models more general than Kolmogorov spectrum in order to describe also non Kolmogorov turbulence. In this paper we use a theoretical spectrum model which reduces to one of Kolmogorov only for a particular case of its exponent: the standard value 11/3. The exponent used here can assume all the values between the range 3 to 4. Using this new spectrum, following the same procedure already used from Andrews and Phillips [1], we have analyzed the impact of the exponent's variation on the a*ngle of arrival fluctuations* for horizontal link in weak turbulence. We have done it for several outer scale values and for different collecting lens radius.

2. NON KOLMOGOROV SPECTRUM

We assume that in an atmosphere exhibiting non-Kolmogorov turbulence the structure function for the index of refraction is given by [1]

Atmospheric Propagation IV, edited by Cynthia Y. Young, G. Charmaine Gilbreath,
Proc. of SPIE Vol. 6551, 65510E, (2007) · 0277-786X/07/$18 · doi: 10.1117/12.719033

$$D_n(R,\gamma) = \beta \cdot C_n^2 \cdot R^{\gamma} \tag{1}$$

where γ is the power law which reduces to 2/3 in the case of conventional Kolmogorov turbulence. Here, β is a constant equal to unity when $\gamma = 2/3$, but otherwise has units $\mathrm{m}^{-\gamma+2/3}$. The corresponding power-law spectrum associated with structure function, as reported in [1][13], takes the form

$$\Phi_n(\kappa,\alpha) = A(\alpha) \cdot \tilde{C}_n^2 \cdot \kappa^{-\alpha}, \quad \kappa > 0,\ 3 < \alpha < 4, \tag{2}$$

where $\alpha = \gamma + 3$ is the spectral index or power law, $\tilde{C}_n^2 = \beta \cdot C_n^2$ is a generalized structure parameter with units $\mathrm{m}^{-\gamma}$, and $A(\alpha)$ is defined by

$$A(\alpha) = \frac{1}{4\pi^2}\Gamma(\alpha-1)\cos\left(\frac{\alpha\pi}{2}\right), \quad 3 < \alpha < 4. \tag{3}$$

where the symbol $\Gamma(x)$ in the last expression is the gamma function.

When $\alpha = 11/3$, we find that $A(11/3) = 0.033$ and the generalized power spectrum reduces to the conventional Kolmogorov spectrum. Also, when the power law approaches the limiting value $\alpha = 3$, the function $A(\alpha)$ approaches zero. Consequently, the refractive-index power spectral density vanishes in this limiting case.

In order to include both inner scale and outer scale effects in (2) we use the follow spectrum

$$\Phi_n(\kappa,\alpha) = A(\alpha) \cdot \tilde{C}_n^2 \cdot \frac{1}{\left(\kappa^2 + \kappa_0^2\right)^{\frac{\alpha}{2}}} \cdot \exp\left(-\frac{\kappa^2}{\kappa_m^2}\right), \quad 0 \le \kappa < \infty,\ 3 < \alpha < 4 \tag{4}$$

where:

- $\kappa_0 = \dfrac{2\pi}{L_0}$, L_0 is outer scale parameter;
- $\kappa_m = \dfrac{c(\alpha)}{l_0}$, l_0 is the inner scale parameter and $c(\alpha) = \left[\Gamma\left(\dfrac{5-\alpha}{2}\right) \cdot A(\alpha) \cdot \dfrac{2}{3}\pi\right]^{\frac{1}{\alpha-5}}$

We obtained the scaling constant $c(\alpha)$ by the procedure showed in Appendix 8.1

Notice that the spectrum (4) reduces to (2) setting $l_0 = 0$ and $L_0 = \infty$. Finally it is interesting to observe that for $\alpha = 11/3$ the spectrum (4) reduces to the (modified) von Kàrmàn spectrum reported in [1].

3. ANGLE OF ARRIVAL ANALYSIS

Angle-of-arrival fluctuations of an optical wave in the plane of the receiver aperture are associated with image dancing in the focal plane of an imaging system. Fluctuations in the angle of arrival β_a can be described in terms of the phase structure function [1]. To understand this, let ΔS denote the total phase shift across a collecting lens of diameter $2W_G$ and Δl the corresponding optical path difference. These quantities are related by

$$k\Delta l = \Delta S \tag{5}$$

If we assume that β_a is small so that $\sin\beta_a \cong \beta_a$, then, under the geometrical optics method (GOM), the angle of arrival is defined by

$$\beta_a = \frac{\Delta l}{2W_G} = \frac{\Delta S}{2kW_G}.[radian] \tag{6}$$

Further assuming the mean $\langle \beta_a \rangle = 0$, we deduce the variance of the angle of arrival

$$\langle \beta_a^{\,2} \rangle = \frac{\langle (\Delta S)^2 \rangle}{(2kW_G)^2} = \frac{D_S(2W_G, L)}{(2kW_G)^2}, \tag{7}$$

where $D_S(2W_G, L)$ is the phase structure function with the radial distance $\rho = 2W_G$.

3.1 Angle of arrival for Plane Wave Model

Following the same procedure as discussed in [1] for the standard Kolmogorov spectrum, but this time using a non-Kolmogorov power spectrum (4), our analysis for plane wave model leads to

$$\begin{aligned} D_{S_{plane}}(\rho, L) &= 8\pi^2 k^2 L \int_0^\infty \kappa \Phi_n(\kappa,\alpha)\cdot\left[1 - J_0(\kappa,\rho)\right] d\kappa \\ &= 4\pi^2 \cdot A(\alpha)\cdot \tilde{C}_n^2 \cdot k^2 \cdot L \cdot \left\{ \kappa_0^{4-\alpha}\cdot\frac{\rho^2}{4}\cdot\frac{\Gamma\left(\frac{\alpha}{2}-2\right)}{\Gamma\left(\frac{\alpha}{2}\right)} + \Gamma\left(1-\frac{\alpha}{2}\right)\cdot\kappa_m^{2-\alpha}\cdot\left[1 - {}_1F_1\left(1-\frac{\alpha}{2};1;-\frac{\kappa_m^2\rho^2}{4}\right)\right]\right\} \end{aligned} \tag{8}$$

where ${}_1F_1(a;b;-z)$ is the Hypergeometric function defined in Appendix 8.2

Replacing $\rho = 2W_G$ and using this approximation that is true for low values of the inner scale parameter l_0

$${}_1F_1(a;c;-z) \cong \frac{\Gamma(c)}{\Gamma(c-a)} z^{-a}, \mathrm{Re}[z] >> 1 \tag{9}$$

we carry out the variance of angle of arrival fluctuations for plane wave model

$$\begin{aligned} \langle \beta_a^2 \rangle_{plane} &= \frac{D_{S_{plane}}(2W_G, L)}{(2kW_G)^2} \\ &= \frac{\pi^2 \cdot A(\alpha)\cdot \tilde{C}_n^2 \cdot L \cdot}{W_G^2} \left\{ \kappa_0^{4-\alpha}\cdot W_G^2 \cdot \frac{\Gamma\left(\frac{\alpha}{2}-2\right)}{\Gamma\left(\frac{\alpha}{2}\right)} + \Gamma\left(1-\frac{\alpha}{2}\right)\cdot\kappa_m^{2-\alpha}\cdot\left[1 - \frac{\left(\kappa_m^2 W_G^2\right)^{\frac{\alpha}{2}-1}}{\Gamma\left(\frac{\alpha}{2}\right)}\right]\right\} \end{aligned} \tag{10}$$

Notice that (10) is independent of optical wavelength, but this is true only if the Fresnel zone is sufficiently small compared with the receiver aperture diameter, $\sqrt{L/k} << 2W_G$.

At this point, we plot the *root mean square* (rms) angle of arrival fluctuations for plane wave $\sqrt{\left\langle \beta_a^2 \right\rangle_{plane}}$ as a function of alpha for a particular horizontal case for several outer scale values. We take
$L = 1km; \tilde{C}_n^2 = 1 \cdot 10^{-14} m^{-\alpha+3}; W_G = 0.05m, l_0 = 0.001m$
The results are shown in figure 1.

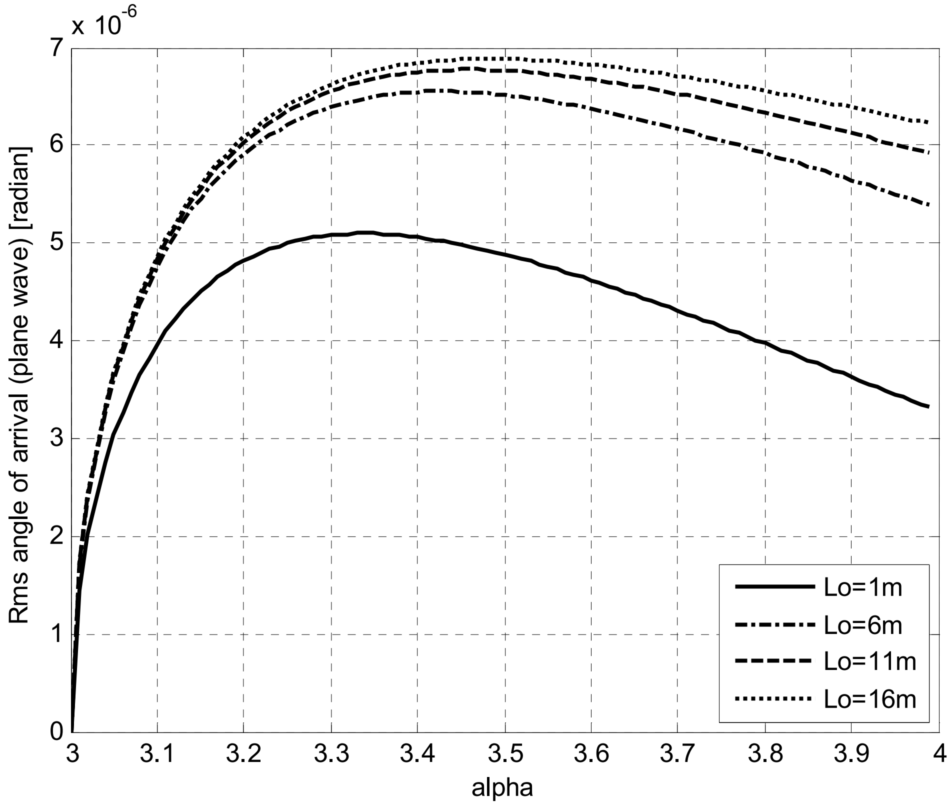

Figure 1- Rms angle of arrival for plane wave as a function of alpha and for different outer scale values

We deduce from figure 1 that rms angle of arrival increases as outer scale increases and it is physically correct. In fact the angle of arrival, like the beam wander, is caused mostly by large-scale turbulence cells, therefore when outer scale assumes high value the laser beam meets a major number of large-scale turbulence cells along its propagation length and these cells leads to higher angle of arrival value with respect to the case of low outer scale value, where more large scale cells are cut out. In addition for alpha value lower than Kolmogorov value $\alpha = 11/3$ angle of arrival increase up to a maximum value. At this maximum point the curve changes its slopes because the term $A(\alpha)$ assumes very low values and rms angle of arrival begins to decrease down to zero. Finally for alpha values higher than Kolmogorov value $\alpha = 11/3$ angle of arrival decreases mostly for low values of the outer scale, instead for high values of the outer scale this decrease tends to vanish.

We plot in figure 2 also a surface of the rms angle of arrival as a function of alpha and outer scale in order to have a three dimensional view of same case.

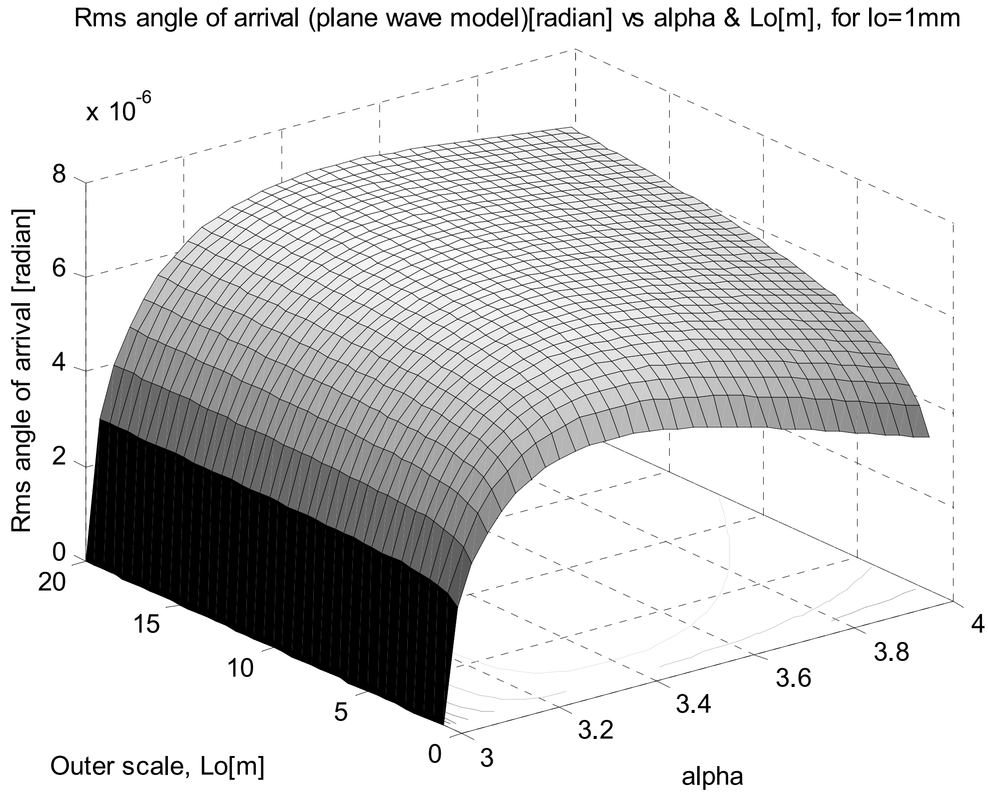

Figure 2 – Rms angle of arrival for plane wave as a function of alpha and outer scale

We plot also rms angle of arrival for plane wave as a function of alpha for a particular horizontal case for several W_G values. We take

$$L = 1km; \tilde{C}_n^2 = 1 \cdot 10^{-14} m^{-\alpha+3}; L_0 = 10m, l_0 = 0.001m$$

The results are shown in figure 3.

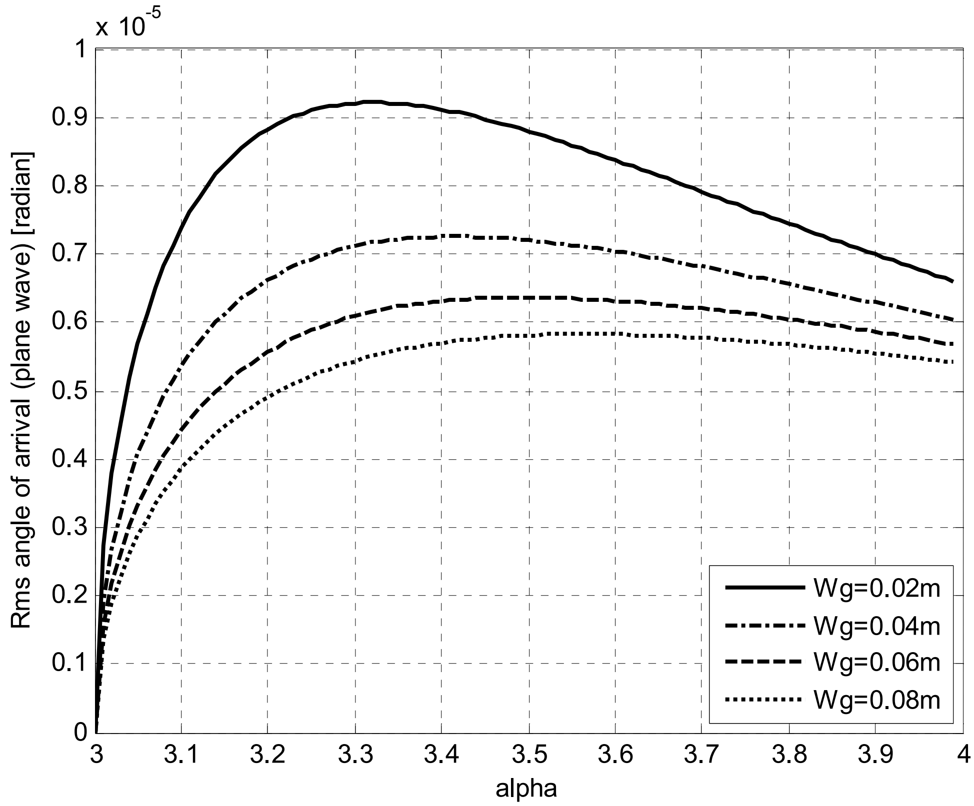

Figure 3 – Rms angle of arrival for plane wave as a function of alpha and for several Wg values

We deduce from figure 3 that alpha variation has different impact on the angle of arrival for different collecting lens radius. In particular if W_G assumes small values there is a bump of the 'rms angle of arrival' for alpha value close to 3.3, instead large values of W_G reduces rms angle of arrival values for every alpha value.

3.2 Spherical Wave Model

Following the same procedure as discussed in [1] for the standard Kolmogorov spectrum, but this time using a non-Kolmogorov spectrum (4), our analysis for spherical wave model leads to

$$\begin{aligned} D_{S_{spherical}}(\rho, L) &= 8\pi^2 k^2 L \int_0^1 \int_0^\infty \kappa \Phi_n(\kappa, \alpha) \cdot \left[1 - J_0(\kappa, \xi, \rho)\right] d\kappa d\xi \\ &= 4\pi^2 \cdot A(\alpha) \cdot \tilde{C}_n^2 \cdot k^2 \cdot L \cdot \left\{ \kappa_0^{4-\alpha} \cdot \frac{\rho^2}{12} \cdot \frac{\Gamma\left(\frac{\alpha}{2} - 2\right)}{\Gamma\left(\frac{\alpha}{2}\right)} + \Gamma\left(1 - \frac{\alpha}{2}\right) \cdot \kappa_m^{2-\alpha} \cdot \left[1 - {}_2F_2\left(1 - \frac{\alpha}{2}, \frac{1}{2}; 1, \frac{3}{2}; -\frac{\kappa_m^2 \rho^2}{4}\right)\right] \right\} \end{aligned} \quad (11)$$

where ${}_2F_2(a, b; c, d; -z)$ is hypergeometric function defined in Appendix 8.3

Replacing $\rho = 2W_G$ and using this approximation that is true for very low values of the inner scale parameter l_0

$$ {}_2F_2\left(a,b;c,d;-z\right) \cong \frac{\Gamma(c)\Gamma(d)\Gamma(b-a)}{\Gamma(b)\Gamma(c-a)\Gamma(d-a)} z^{-a}, z \to \infty, a < b \tag{12} $$

We carry out angle of arrival expression for spherical wave model

$$ \begin{aligned} \left\langle \beta_a^2 \right\rangle_{spherical} &= \frac{D_{S_{plane}}\left(2W_G, L\right)}{\left(2kW_G\right)^2} = \frac{\pi^2 \cdot A(\alpha) \cdot \tilde{C}_n^2 \cdot L}{W_G^2} \cdot \\ &\times \left\{ \frac{\kappa_0^{4-\alpha} \cdot W_G^2}{3} \cdot \frac{\Gamma\left(\frac{\alpha}{2}-2\right)}{\Gamma\left(\frac{\alpha}{2}\right)} + \Gamma\left(1-\frac{\alpha}{2}\right) \cdot \kappa_m^{2-\alpha} \cdot \left(1 - \frac{\Gamma\left(\frac{3}{2}\right)\Gamma\left(\frac{\alpha-1}{2}\right) \cdot \kappa_m^{\alpha-2} \cdot W_G^{\alpha-2}}{\Gamma\left(\frac{1}{2}\right)\Gamma\left(\frac{\alpha}{2}\right)\Gamma\left(\frac{1+\alpha}{2}\right)} \right) \right\}, \kappa_m >> 0 \end{aligned} \tag{13} $$

Notice that, like for plane wave model case, (13) is independent of optical wavelength, but this is true only if the Fresnel zone is sufficiently small compared with the receiver aperture diameter, $\sqrt{L/k} << 2W_G$.

At this point, we plot the *root mean square* (rms) angle of arrival fluctuations for spherical wave, $\sqrt{\left\langle \beta_a^2 \right\rangle_{spherical}}$, as a function of alpha for a particular horizontal case for several outer scale values. We take

$$ L = 1km; \tilde{C}_n^2 = 1 \cdot 10^{-14} m^{-\alpha+3}; W_G = 0.05m, l_0 = 0.001m $$

The results are shown in figure 4.

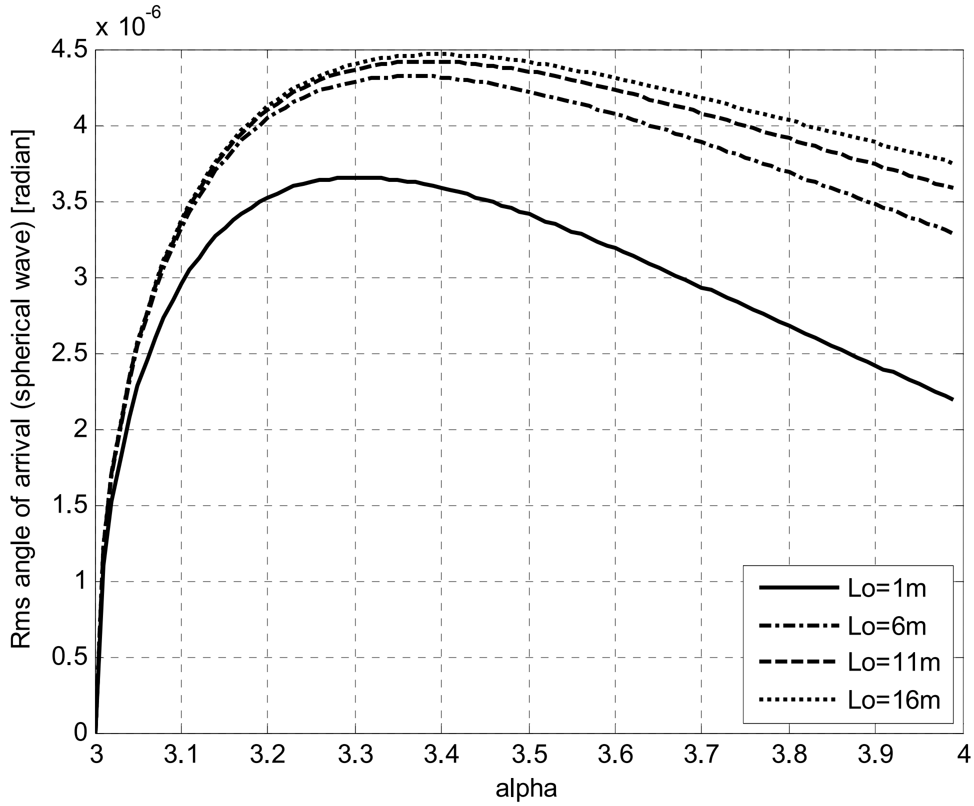

Figure 4– Rms angle of arrival for spherical wave as a function of alpha and for several outer scale values

We deduce from figure 4 the same comments as for figure 1. However, setting the same parameters, rms angle of arrival values for plane wave model are higher than angle of arrival values for spherical wave model.
We plot in figure 5 also a surface of rms angle of arrival as a function of alpha and outer scale in order to have a three dimensional view of same case.

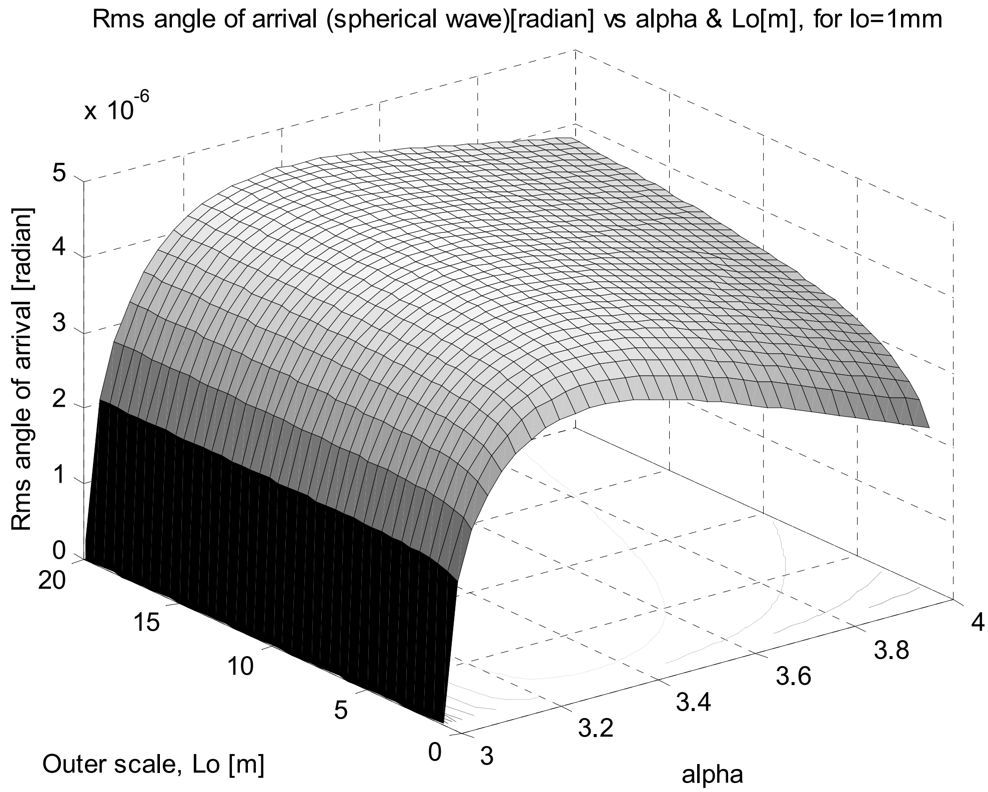

Figure 5 – Rms angle of arrival for spherical wave as a function of alpha and of the outer scale for horizontal path

We plot also rms angle of arrival for spherical wave as a function of alpha for a particular horizontal case for several W_G values. We take

$$L = 1km; \tilde{C}_n^2 = 1 \cdot 10^{-14} m^{-\alpha+3}; L_0 = 10m, l_0 = 0.001m$$

The results are shown in figure 6.

We deduce from figure 6 the same comments as for figure 3.

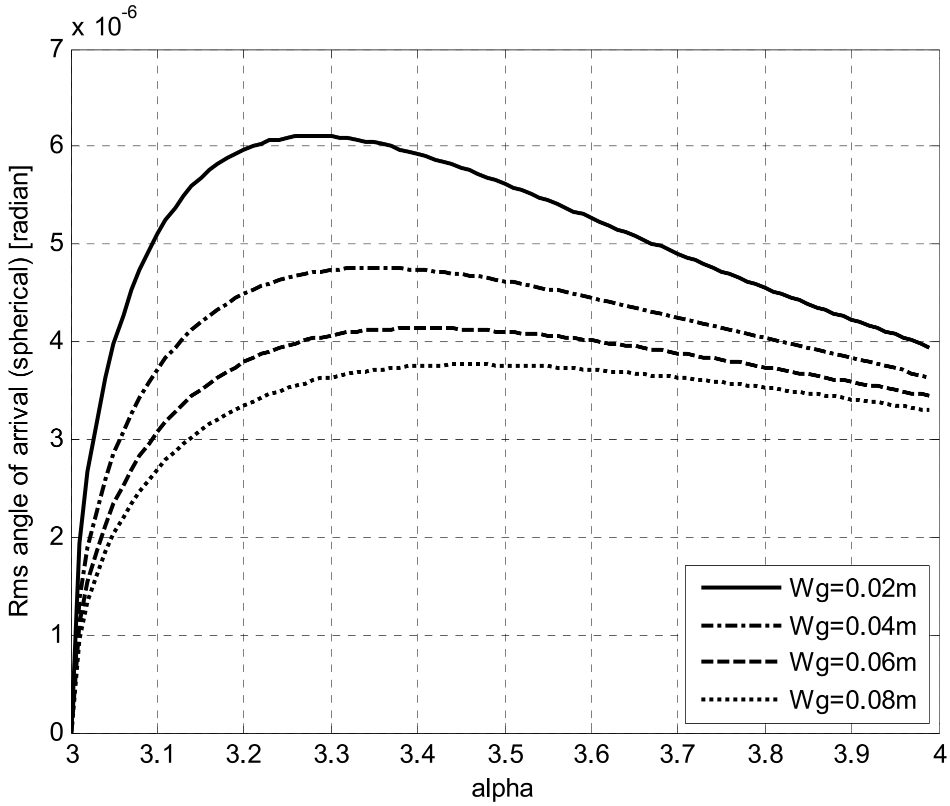

Figure 6 – Rms angle of arrival for spherical wave as a function of alpha for horizontal path and for several Wg values

4. DISCUSSION

In this paper we have analyzed angle of arrival fluctuation using a non-Kolmogorov power spectrum, which uses both a generalized exponent and a generalized amplitude factor instead of a constant standard exponent value $\alpha = 11/3$ and a constant amplitude factor 0.033 such is for Kolmogorov spectrum. This non-Kolmogorov spectrum has been carried out from a generalized structure function. It has been shown for horizontal path, in weak turbulence, angle of arrival as variation of alpha exponent that assumes values around the standard value of Kolmogorov $\alpha = 11/3$.

Both for plane wave model and spherical wave model, it has been shown that for alpha values lower than Kolmogorov value $\alpha = 11/3$ the rms angle of arrival increases up to a maximum value. At these maximum points the curves changes their slopes because the term $A(\alpha)$ assumes very low values and rms angle of arrival begins to decrease down to zero. In addition for alpha values higher than Kolmogorov value $\alpha = 11/3$ the rms angle of arrival decreases especially for low values of the outer scale, instead for high values of the outer scale this decrease tends to vanish. Finally it has been shown that alpha variation has different impact on the angle of arrival for different collecting lens radius. In particular if W_G assumes small values there is a bump of the angle of arrival for alpha value close to 3.3, instead large values of W_G reduces angle of arrival values for every alpha value.

8. APPENDIX

8.1 Non Kolmogorov spectrum: c(α) scaling constant evaluation procedure

The structure function is given by [1]

$$D_n(R,\alpha) = 8\pi \int_0^\infty \kappa^2 \cdot \Phi_n(\kappa,\alpha) \cdot \left(1 - \frac{\sin \kappa R}{\kappa R}\right) d\kappa$$

By using the spectrum (4) with $\kappa_0 = 0$ and retaining the first non zero term of the Maclaurin series representation

$$1 - \frac{\sin \kappa R}{\kappa R} = \sum_1^\infty \frac{(-1)^{n-1}}{(2n+1)!} \kappa^{2n} R^{2n}$$

we carry out

$$D_n(R,\alpha) = \frac{2}{3}\pi \cdot \Gamma\left(5 - \frac{\alpha}{2}\right) \cdot A(\alpha) \cdot \tilde{C}_n^2 \cdot R^2 \cdot \kappa_m^{5-\alpha}$$

By assuming $\kappa_m = \dfrac{c(\alpha)}{l_0}$ and using the asymptotic behavior of the structure function [1]

$$D_n(R,\alpha) = \tilde{C}_n^2 \cdot l_0^{\alpha-5} \cdot R^2, \qquad 0 \le R << l_0$$

we deduce $c(\alpha) = \left[\Gamma\left(\dfrac{5-\alpha}{2}\right) \cdot A(\alpha) \cdot \dfrac{2}{3}\pi\right]^{\frac{1}{\alpha-5}}$

8.2 Confluent Hypergeometric Functions of the first kind

The series representation for the confluent hypergeometric function [1][14] of the first kind is given by

$${}_1F_1(a;b;z) = \sum_0^\infty \frac{(a)_n}{(b)_n} \cdot \frac{z^n}{n!}, |z| < \infty$$

where z may be real or complex.

8.3 Generalized Hypergeometric Functions

The series representation for the generalized hypergeometric function [1][14] is given by

$${}_2F_2(a,b;c,d;z) = \sum_0^\infty \frac{(a)_n \cdot (b)_n}{(c)_n \cdot (d)_n} \cdot \frac{z^n}{n!}, |z| < \infty$$

9. REFERENCES

1. Larry C. Andrews, Ronald L. Phillips. *Laser Beam Propagation through Random Media*. Spie Press, second edition - 2005.
2. Larry C. Andrews, Ronald L. Phillips, Cynthia Y. Hopen. *Laser Beam Scintillation with Applications*. Spie Press, 2001.
3. David Dayton, Bob Pierson, Brian Spielbusch. *Atmospheric structure function measurements with a Shack-Hartmann wave front sensor.* Optics letters ,vol.17, num. 24,1992.
4. J. McWilliam, Phys. Fluids, A 2, 547, 1990.
5. Mikhail S. Be1enkii, Stephen J. Karis, James M. Brown II, and Robert Q. Fugate. *Experimental study of the effect of non-Kolmogorov stratospheric turbulence on star image motion.* SPIE vol. 3126, 1997.
6. Ephim Golbraikh, Norman S. Kopeika. *Behavior of structure function of refraction coefficients in different turbulent fields.* Applied Optics, vol 43, num. 33, 2004.
7. Gregory Falkovich, Katepalli R. Sreenivasan. *Lessons from Hydrodynamic Turbulence*. Physics Today, April 2006.
8. A I Kon. *Qualitative theory of amplitude and phase fluctuations in a medium with anisotropic turbulent irregularities.* Wave in random media 4, 297-305, 1994.
9. Bruce E. Stribling, Byron M. Welsh and Michael C. Roggemann. *Optical propagation in non-Kolmogorov Atmospheric Turbulence.* SPIE vol.2471, 181-196, 1995.
10. Demos T. Kyrazis, John Wissler, Donna D.B. Keating, Amanda J.Preble, Kenneth P. Bishop. *Measurement of optical turbulence in the upper troposphere and lower stratosphere.* SPIE vol. 2110, 1994.
11. Mikhail S. Belen'kii, Stephen J.Karis, Christian L. Osmon. *Experimental evidence of the effects of non-Kolmogorov turbulence and anisotropy of turbulence.* SPIE vol. 3749, 1999.
12. Robert R. Beland, *Some aspects of propagation through weak isotropic non-Kolmogorov turbulence.* SPIE vol. 2375, 1995.
13. Italo Toselli, Larry C. Andrews, Ronald L. Phillips, Valter Ferrero. *Free space optical system performance for laser beam propagation through non Kolmogorov turbulence*. SPIE vol.6457, 2007.
14. Larry C. Andrews. *Special functions of mathematics for engineers.* Spie Press, second edition – 1997.